JAERI-M
87-008

ENERGY CONFINEMENT AND PROFILE CHARACTERISTICS DURING THE INITIAL NEUTRAL BEAM HEATING IN JT-60

February 1987

Mitsuru KIKUCHI, Toshio HIRAYAMA, Katsuhiro SHIMIZU
Keiji TANI, Hidetoshi YOSHIDA, Hideaki YOKOMIZO
Takeshi FUKUDA, Akira SAKASAI, Yoshihiko KOIDE
Tatsuo SUGIE, Hiroshi HORIIKE, Masaaki KURIYAMA
Hiromasa NINOMIYA, Nobuyuki HOSOGANE, Ryuji YOSHINO
and JT-60 team

日本原子力研究所
Japan Atomic Energy Research Institute

JAERI-Mレポートは，日本原子力研究所が不定期に公刊している研究報告書です。
入手の問合わせは，日本原子力研究所技術情報部情報資料課（〒319-11 茨城県那珂郡東海村）あて，お申しこしください。なお，このほかに財団法人原子力弘済会資料センター（〒319-11 茨城県那珂郡東海村日本原子力研究所内）で複写による実費頒布をおこなっております。

JAERI-M reports are issued irregularly.
Inquiries about availability of the reports should be addressed to Information Division Department of Technical Information, Japan Atomic Energy Research Institute, Tokaimura, Naka-gun, Ibaraki-ken 319-11, Japan.

編集兼発行　日本原子力研究所
印　　　刷　日青工業株式会社

Energy Confinement and Profile Characteristics during the Initial Neutral Beam Heating in JT-60

Mitsuru KIKUCHI, Toshio HIRAYAMA, Katsuhiro SHIMIZU, Keiji TANI, Hidetoshi YOSHIDA, Hideaki YOKOMIZO, Takeshi FUKUDA, Akira SAKASAI, Yoshihiko KOIDE, Tatsuo SUGIE, Hiroshi HORIIKE, Masaaki KURIYAMA, Hiromasa NINOMIYA, Nobuyuki HOSOGANE, Ryuji YOSHINO
and JT-60 team

Department of Large Tokamak Research
Naka Fusion Research Establishment
Japan Atomic Energy Research Institute
Naka-machi, Naka-gun, Ibaraki-ken

(Received January 19, 1987)

Confinement results are reported during the 3 months initial operation of JT-60 tokamak with I_p of 1-2 MA, $\bar{n}_e$ of $1.5\text{-}7\times10^{19}m^{-3}$ and P_{abs} up to 20MW. The plasma stored energy follows an offset linear relation with the absorbed power and the incremental energy confinement time τ_E^{inc} $(=dW_s/dP_{abs})$ for thermal components is almost independent of I_p and $\bar{n}_e$ and is 60 msec. A remarkable difference in the density profile has been observed between limiter and divertor discharges. The electron temperature profile shape is rather tight compared with the density profile although broader profiles have been observed in high density beam heated discharges.

Keywords: Energy Confinement, JT-60, Plasma Stored Energy, Profile Consistency, Neutral Beam Heating

JT-60 team

T. ABE, H. AIKAWA, N. AKAOKA, H. AKASAKA, M. AKIBA, N. AKINO, T. AKIYAMA,
T. ANDO, K. ANNOH, N. AOYAGI, T. ARAI, K. ARAKAWA, M. ARAKI, K. ARIMOTO,
M. AZUMI, S. CHIBA, M. DAIRAKU, N. EBISWA, T. FUJII, T. FUKUDA, H. FURUKAWA,
K. HAMAMATSU, K. HAYASHI, M. HARA, K. HARAGUCHI, H. HIRATSUKA, T. HIRAYAMA,
S. HIROKI, K. HIRUTA, M. HONDA, H. HORIIKE, R. HOSODA, N. HOSOGANE, Y. IIDA,
T. IIJIMA, K. IKEDA, Y. IKEDA, T. IMAI, T. INOUE , N. ISAJI, M. ISAKA,
S. ISHIDA, N. ITIGE, T. ITO, Y. ITO, A. KAMINAGA, M. KAWAI, Y. KAWAMATA,
K. KAWASAKI, K. KIKUCHI, M. KUKUCHI, H. KIMURA, T. KIMURA, H. KISHIMOTO,
K. KITAHARA, S. KITAMURA, A. KITSUNEZAKI, K. KIYONO, N. KOBAYASHI,
K. KODAMA, Y. KOIDE, T. KOIKE, M. KOMATA, I. KONDO, S. KONOSHIMA, H. KUBO,
S. KUNIEDA, S. KURAKATA, K. KURIHARA, M. KURIYAMA, T. KURODA, M. KUSAKA,
Y. KUSAMA, S. MAEHARA, K. MAENO, S. MATSUDA, S. MASE, M. MATSUKAWA.
T. MATSUKAWA, M. MATSUOKA, N. MIYA, K. MIYATI, Y. MIYO, K. MIZUHASHI,
M. MIZUNO, R. MURAI, Y. MURAKAMI, M. MUTO, M. NAGAMI, A. NAGASHIMA,
K. NAGASHIMA, T. NAGASHIMA. S. NAGAYA, H. NAKAMURA, Y. NAKAMURA, M. MEMOTO,
Y. NEYATANI, S. NIIKURA, H. NINOMIYA, T. NISHITANI, H. NOMATA, K. OBARA,
N. OGIWARA, T. OHGA, Y. OHARA, K. OHASA, H. OHHARA, T. OHSHIMA, M. OHKUBO,
K. OHTA, M. OHTA, M. OHTAKA, Y. OHUCHI, A. OKIKAWA, H. OKUMURA, Y. OKUMURA,
K. OMORI, S. OMORI, Y. OMORI, T. OZEKI, A. SAKASAI, S. SAKATA, M. SATOU,
M. SAIGUSA, K. SAKAMOTO, M. SAWAHATA, M. SEIMIYA, M. SEKI, S. SEKI,
K. SHIBANUMA, R. SHIMADA, K. SHIMIZU, M. SHIMIZU, Y. SHIMOMURA, S. SHINOZAKI,
H. SHIRAI, H. SHIRAKATA, M. SHITOMI, K. SUGANUMA, T. SUGIE, T. SUGIYAMA,
H. SUNAOSHI, K. SUZUKI, M. SUZUKI, M. SUZUKI, N. SUZUKI, S. SUZUKI, Y. SUZUKI,
M. TAKAHASHI, S. TAKAHASHI, T. TAKAHASHI, H. TAKAHASHI**, M. TAKASAKI,
M. TAKATSU, H. TAKEUCHI, A. TAKESHITA, S. TAMURA, S. TANAKA, T. TANAKA,
K. TANI, M. TERAKADO, T. TERAKADO, K. TOBITA, T. TOKUTAKE, T. TOTSUKA,
N. TOYOSHIMA, H. TSUDA, T. TSUGITA, S. TSUJI, Y. TSUKAHARA, M. TSUNEOKA,
K. UEHARA, M. UMEHARA, Y. URAMOTO, U. USAMI, K. UCHIGUSA, K. USUI, J. YAGYU,
K. YAMADA, M. YAMAMOTO. O. YAMASHITA, Y. YAMASHITA, K. YANO, T. YASUKAWA,
K. YOKOKURA, H. YOKOMIZO, K. YOSHIKAWA, M. YOSHIKAWA, H. YOSHIDA,
Y. YOSHINARI, R. YOSHINO, I. YONEKAWA, K. WATANABE

ＪＴ－60の初期ＮＢＩ加熱時のエネルギー閉じ込めと分布特性

日本原子力研究所那珂研究所臨界プラズマ研究部
菊池　満・平山　俊雄・清水　勝宏・谷　啓二・吉田　英俊
横溝　英明・福田　武司・逆井　章・小出　芳彦・杉江　達夫
堀池　寛・栗山　正明・二宮　博正・細金　延幸・芳野　隆治
ＪＴ－60チーム

（1987年1月19日受理）

ＪＴ－60の３ケ月間の初期ＮＢＩ加熱（$I_P = 1 \sim 2$ MA，$\overline{n}_e = 1.5 \sim 7 \times 10^{19} m^{-3}$，$P_{abs} \leq$ 20MＷ）のエネルギー閉じ込め特性を報告する。プラズマ蓄積エネルギーは吸収パワーに対してオフセットをもって線形に増大する。また，熱エネルギー増分に対するエネルギー閉じ込め時間$\tau_E^{inc}(=\frac{dW_s}{dP_{abs}})$は$I_P$，$\overline{n}_e$によらず60msecである。リミター放電とダイバータ放電の間で，著しい密度分布の差が観測された。電子温度分布は密度分布に比べると比較的変わりにくい。但し，高密度域で多少分布が広がる傾向が見られた。

那珂研究所：〒311-02 茨城県那珂郡那珂町大字向山 801－1

相川 裕史, 青柳 哲雄, 赤岡 伸雄, 赤坂 博美, 秋野 昇, 秋場 真人,
秋山 隆, 安積 正史, 阿部 哲也, 新井 貴, 荒川喜代次, 荒木 政則,
有本 公子, 安東 俊郎, 安納 勝人, 飯島 勉, 飯田 幸生, 池田 幸治,
池田 佳隆, 井坂 正義, 伊佐治信明, 石田 真一, 市毛 尚志, 伊藤 孝雄,
伊藤 康浩, 井上多加志, 今井 剛, 上原 和也, 宇佐美広次, 牛草 健吉,
薄井 勝富, 梅原 昌敏, 浦本 保幸, 海老沢 昇, 及川 晃, 大麻 和美,
大内 豊, 大賀 徳道, 大久保 実, 大島 貴幸, 太田 和也, 太田 充,
大高 光夫, 大原比呂志, 大森憲一郎, 大森 俊造, 大森 栄和, 荻原 徳男,
奥村 裕司, 奥村 義和, 小関 隆久, 小原建治郎, 小原 祥裕, 神永 敦嗣,
河合視己人, 川崎 幸三, 川俣 陽一, 菊池 勝美, 菊池 満, 岸本 浩,
北原 勝美, 北村 繁, 狐崎 晶雄, 木村 豊秋, 木村 晴行, 清野 公廣,
日下 誠, 草間 義紀, 国枝 俊介, 久保 博孝, 倉形 悟, 栗原 研一,
栗山 正明, 黒田 猛, 小池 常之, 小出 芳彦, 児玉 幸三, 木島 滋,
小林 則幸, 小又 将夫, 近藤 育朗, 三枝 幹雄, 逆井 章, 坂田 信也,
坂本 慶司, 佐藤 正泰, 沢畠 正之, 蔀 守正, 篠崎 信一, 芝沼 清,
嶋田 隆一, 清水 勝宏, 清水 正亜, 下村 安夫, 白井 浩, 白形 弘文,
菅沼 和明, 杉江 達夫, 杉山 隆, 鈴木 貞明, 鈴木 國弘, 鈴木 紀男,
鈴木 正信, 鈴木 道雄, 鈴木 康夫, 砂押 秀則, 清宮 宗孝, 関 省吾,
関 正美, 高崎 学, 高津 英美, 高橋 春次, 高橋虎之助, 高橋 弘法,
高橋 実, 竹内 浩, 竹下 明, 田中 茂, 田中竹次郎, 谷 啓二,
田村 早苗, 大楽 正幸, 千葉 真一, 塚原 美光, 次田 友宣, 辻 俊二,
津田 文男, 恒岡まさき, 寺門 恒久, 寺門 正之, 徳竹 利国, 戸塚 俊之,
飛田 健次, 豊島 昇, 中村 博雄, 中村 幸治, 長島 章, 永島 圭介,
永島 孝, 永島 進, 永見 正幸, 新倉 節夫, 西谷 健夫, 二宮 博正,
根本 正博, 閨谷 譲, 野亦 英幸, 濱松 清隆, 林 和夫, 原 誠,
原口 和三, 平塚 一, 平山 俊雄, 蛭田 和治, 広木 成治, 福田 武司,
藤井 常幸, 古川 弘, 細金 延幸, 細田隆一郎, 堀池 寛, 本田 正男,
前野 勝樹, 前原 直, 間瀬 修次, 松岡 守, 松川 達哉, 松川 誠,
松田慎三郎, 水野 誠, 水橋 清, 宮 直之, 宮地 謙吾, 三代 康彦,
武藤 貢, 村井 隆一, 村上 義夫, 柳生 純一, 安川 亨, 矢野 勝久,
山下 修, 山下 幸彦, 山田喜美雄, 山本 正弘, 横倉 賢治, 横溝 英明,
吉川 和伸, 吉川 允二, 吉田 英俊, 吉成 洋治, 芳野 隆治, 米川 出,
渡辺 和弘,

Contents

目　　次

1. INTRODUCTION

The research objective of JT-60 is to achieve and study reactor relavant plasmas ($\overline{n}_e\tau_E$=2-6x10$^{19}m^{-3}$ and T_i = 5-10 kev) [1] . In order to realize such a plasma condition, neutral beam power up to 20 MW has been injected into 2 MA divertor discharges [2,3,4,5] in JT-60. Extensive studies have been made during ohmic heating experiments to get a wide range of target plasma density before auxiliary heating in JT-60 [6,7,8,9] .

More than 10 years of experimental efforts have been paid to get the empirical confinement scaling during the auxiliary heating. Based on early experimental results, Goldston [10] suggested an empirical scaling for the global energy confinement time for so called L-mode. Later Kaye and Goldston proposed a refined energy confinement scaling [11] . Both Goldston and Kaye-Goldston scalings gave rough agreement with the L-mode confinement for present large tokamak experiments such as TFTR, JET and JT-60 [12,13,2] . They basically assumed the global energy confinement time can be expressed by the multiple power fit of the externally controllable parameters such as $I_p, \overline{n}_e, B_t, P_{tot}, R_p, a_p, \kappa$. Offset inverse linear dependence has been proposed as an alternative approach for the power dependence of the energy confinement time by Burrell [14] and DeBoo [15] . More recently, Odajima [16] showed that τ_E^{inc} is independent of $I_p, \overline{n}_e$ and P_{abs} in JFT-2M and the size scaling part of the incremental energy confinement time is obtained by Shimomura and Odajima [17] .

It has been well understood that different physical mechanisms rule the energy confinement properties of ohmic and neutral beam heated L-mode discharges. Goldston showed that confinement properties of both ohmic and beam-heated discharges is well described by the combination of 2 independent confinement times τ_E^{OH} and τ_E^{AUX} while Odajima divided plasma stored energy into 2 terms W_{OH} and ΔW^{inc} which follow different confinement scalings τ_E^{OH} and τ_E^{inc} , respectively.

In order to understand the underlying physics of tokamak confinement, there are growing discussions on the profile constraints originating from Coppi's "Principle of Profile Consistency" [18] . This guiding philosophy simply means that transport coefficients such as D and χ are not locally defined but are determined from the global profile constraint. Such profile constraint may be related to the fact that both central and edge temperatures are constrained by the sawteeth and the high neutral recycling at plasma edge, respectively. The profile invariance or tightness has been shown by Murakami [19] and Speth [20] during the neutral beam heating.

In this paper, we will show the energy confinement properties and T_e and n_e profile characteristics during the hydrogen neutral beam heated L-mode discharges in JT-60.

2. EXPERIMENTAL CONDITIONS AND DIAGNOSTICS

JT-60 is a large tokamak which can produce near circular limiter and divertor plasmas. The basic machine conditions for the experiments described in this paper are nearly same as the nominal design value for the divertor operation in JT-60 [8] . Most of the experimental data are obtained in the divertor discharges. The divertor configuration of JT-60 is characterized by the location of the x point. Arrangement of diagnostics system for energy confinement and typical divertor equilibrium are shown in Fig.1. 4 channel interferometer system is used to estimate the radial profile of the electron density. Radial profile of the electron temperature and density is measured by the 6 points Thomson scattering system shown in the figure. Central electron temperature measured by a soft-X-ray pulse height analyzer is in good agreement with the Thomson scattering values. Central ion temperature is measured by the doppler broadening of the T_i XXI K_α line, Rutherford scattering of the diagnostics helium beam and charge exchange neutral analyzer. Total radiation from the plasma is measured by the 15 channel bolometer array. Z_{eff} is estimated by the visible bremsstrahlung, Rutherford scattering of diagnostics helium beam and the resistivity.

Prior to the experiment, extensive Taylor type discharge conditioning has been made to reduce impurity influx [21] . The plasma is initiated in a limiter condition and is changed into the guiding philosophy simply means that transport coefficients such as D and χ are not locally defined but are determined from the global profile constraint. Such profile constraint may be related to the fact that both central and edge temperatures are constrained by the sawteeth and the high neutral recycling at plasma edge, respectively. The profile invariance or tightness has been shown by Murakami [19] and Speth [20] during the neutral beam heating.

In this paper, we will show the energy confinement properties and T_e and n_e profile characteristics during the hydrogen neutral beam heated L-mode discharges in JT-60.

2. EXPERIMENTAL CONDITIONS AND DIAGNOSTICS

JT-60 is a large tokamak which can produce near circular limiter and divertor plasmas. The basic machine conditions for the experiments described in this paper are nearly same as the nominal design value for the divertor operation in JT-60 [8] . Most of the experimental data are obtained in the divertor discharges. The divertor configuration of JT-60 is characterized by the location of the x point. Arrangement of diagnostics system for energy confinement and typical divertor equilibrium are shown in Fig.1. 4 channel interferometer system is used to estimate the radial profile of the electron density. Radial profile of the electron temperature and density is measured by the 6 points Thomson scattering system shown in the figure. Central electron temperature measured by a soft-X-ray pulse height analyzer is in good agreement with the Thomson scattering values. Central ion temperature is measured by the doppler broadening of the T_i XXI K_α line, Rutherford scattering of the diagnostics helium beam and charge exchange neutral analyzer. Total radiation from the plasma is measured by the 15 channel bolometer array. Z_{eff} is estimated by the visible bremsstrahlung, Rutherford scattering of diagnostics helium beam and the resistivity.

Prior to the experiment, extensive Taylor type discharge conditioning has been made to reduce impurity influx [21] . The plasma is initiated in a limiter condition and is changed into the divertor configuration after around 200 msec. Feedback control of Δ_R and Δ_Z is started 60 msec after the initiation of the discharge. Active feedback control analysis, configuration measurement and initial control results are seen in the references [22,23,24] . Fig.2 shows a typical discharge characteristics during the neutral beam heating in JT-60. All confinement data are taken near the end of the neutral beam pulse where the discharge is nearly stationary.

3. ANALYSIS PROCEDURES

The diagnostics data obtained in the experiments are analyzed by the time independent analysis code LOOK/OFMC/SCOOP developed in JAERI [25] which is similar to ZORNOC [26] and SNAP [19] . The analysis procedure is schematically shown in Fig.3. Outermost flux surface is obtained by using FBI(Fast Boundary Identification) code [27] which uses the same method developed by Swain [28] . Internal flux surface is calculated by the numerical equilibrium code using the fixed boundary condition from FBI code. Electron density and temperature profiles are determined as a function of ψ. The density and temperature profiles can be well described by the following forms in JT-60,

$$n_e(r) = (n_e(0) - n_{eb})(1-(r/a)^2)^m + n_{eb}$$

$$T_e(r) = (T_e(0) - T_{eb})\{1-(r/a)^2 + \alpha(r/a)^2(1-r/a) + \beta(r/a)^2(1-(r/a)^2)\} + T_{eb}$$

and the unknown parameters are obtained by the least square fit to the measurements. Radiation profile can be obtained as a function of ψ by inversion of the 15 channel chord measurement. It should be noted that total radiation measured by the 15 channel bolometer array is only 5-10 % of total absorbed power and it does not play a major role in the power balance. Radiation profile is rather flat except small peaks at the center and the edge and we simply assumed flat profile for the power balance study. Energy and particle deposition profiles from the neutral beam is calculated by the OFMC(Orbit-Following-Monte-Carlo) code [29] . Radial profiles of the transport coefficients D and χ and power divertor configuration after around 200 msec. Feedback control of Δ_R and Δ_Z is started 60 msec after the initiation of the discharge. Active feedback control analysis, configuration measurement and initial control results are seen in the references [22,23,24] . Fig.2 shows a typical discharge characteristics during the neutral beam heating in JT-60. All confinement data are taken near the end of the neutral beam pulse where the discharge is nearly stationary.

3. ANALYSIS PROCEDURES

The diagnostics data obtained in the experiments are analyzed by the time independent analysis code LOOK/OFMC/SCOOP developed in JAERI [25] which is similar to ZORNOC [26] and SNAP [19] . The analysis procedure is schematically shown in Fig.3. Outermost flux surface is obtained by using FBI(Fast Boundary Identification) code [27] which uses the same method developed by Swain [28] . Internal flux surface is calculated by the numerical equilibrium code using the fixed boundary condition from FBI code. Electron density and temperature profiles are determined as a function of ψ. The density and temperature profiles can be well described by the following forms in JT-60,

$$n_e(r) = (n_e(0) - n_{eb})(1-(r/a)^2)^m + n_{eb}$$

$$T_e(r) = (T_e(0) - T_{eb})\{1-(r/a)^2 + \alpha(r/a)^2(1-r/a) + \beta(r/a)^2(1-(r/a)^2)\} + T_{eb}$$

and the unknown parameters are obtained by the least square fit to the measurements. Radiation profile can be obtained as a function of ψ by inversion of the 15 channel chord measurement. It should be noted that total radiation measured by the 15 channel bolometer array is only 5-10 % of total absorbed power and it does not play a major role in the power balance. Radiation profile is rather flat except small peaks at the center and the edge and we simply assumed flat profile for the power balance study. Energy and particle deposition profiles from the neutral beam is calculated by the OFMC(Orbit-Following-Monte-Carlo) code [29] . Radial profiles of the transport coefficients D and χ and power flow, and global confinement parameters are calculated in SCOOP code.

Physical assumptions for the confinement analysis are as follows. The ion temperature profile is estimated by assuming $\chi_i = = C_i\ \chi_i^{NC}$ where C_i and χ_i^{NC} are the 'neoclassical multiplier' and the neoclassical ion thermal conductivity given by Chang-Hinton [30] C_i is determined from the measured central ion temperature. $C_i = 5$ is assumed in high density discharges without using the measured ion temperature where small differences between ion and electron temperatures are expected. The beam component of the plasma stored energy is estimated by the Orbit-Follwing-Monte-Carlo code which increases with P_{NB} and decreases with $\bar{n}_e$. Beam component of the stored energy is typically 20 % of the total stored energy at $\bar{n}_e$=3x10$^{19}m^{-3}$. No anomalous loss mechanism for the beam component is included in the calculation such as fishbone instability.

4. ENERGY CONFINEMENT DURING THE BEAM HEATING

Energy confinement characteristics of ohmically heated plasma has been analyzed which is important for the description of the 'incremental energy confinement time' during the neutral beam heating. Fig.4 shows the plasma stored energy as a function of $\bar{n}_e$ for various plasma currents. Plasma stored energy is well described by the following formula,

$$W_s^{OH} = 0.157\ I_p(\mathrm{MA})^{0.86}\ \bar{n}_e^{0.62}\ (10^{19}\ m^{-3})$$

Fig.5 shows the total kinetic stored energy W_{TOT} (= $W_e + W_i + W_b$) as a function of absorbed power P_{abs} (=$P_{NBI} - P_{ST} + P_{OH}$) where W_e, W_i, W_b, P_{NBI}, P_{ST} and P_{OH} are electron stored energy, ion stored energy, beam stored energy, neutral injection power, shine through power and joule heating power, respectively. Both hydrogen and helium discharge data are included in the figure because no significant difference in the confinement properties have been observed. The density ranges are restricted to 4-5 x 10$^{19}m^{-3}$ for I_p=2 MA case and 3.4-4.0 x 10$^{19}m^{-3}$ for I_p=1.5 MA case because the stored energy has a strong dependence on the flow, and global confinement parameters are calculated in SCOOP code.

Physical assumptions for the confinement analysis are as follows. The ion temperature profile is estimated by assuming $\chi_i = C_i \chi_i^{NC}$ where C_i and χ_i^{NC} are the "neoclassical multiplier" and the neoclassical ion thermal conductivity given by Chang-Hinton [30] C_i is determined from the measured central ion temperature. $C_i = 5$ is assumed in high density discharges without using the measured ion temperature where small differences between ion and electron temperatures are expected. The beam component of the plasma stored energy is estimated by the Orbit-Follwing-Monte-Carlo code which increases with P_{NB} and decreases with $\bar{n}_e$. Beam component of the stored energy is typically 20 % of the total stored energy at $\bar{n}_e$=3x10$^{19}m^{-3}$. No anomalous loss mechanism for the beam component is included in the calculation such as fishbone instability.

4. ENERGY CONFINEMENT DURING THE BEAM HEATING

Energy confinement characteristics of ohmically heated plasma has been analyzed which is important for the description of the "incremental energy confinement time" during the neutral beam heating. Fig.4 shows the plasma stored energy as a function of $\bar{n}_e$ for various plasma currents. Plasma stored energy is well described by the following formula,

$$W_s^{OH} = 0.157\ I_p(\mathrm{MA})^{0.86}\ \bar{n}_e^{0.62}\ (10^{19}\ \mathrm{m}^{-3})$$

Fig.5 shows the total kinetic stored energy W_{TOT} (= $W_e + W_i + W_b$) as a function of absorbed power P_{abs} (=$P_{NBI} - P_{ST} + P_{OH}$) where W_e, W_i, W_b, P_{NBI}, P_{ST} and P_{OH} are electron stored energy, ion stored energy, beam stored energy, neutral injection power, shine through power and joule heating power, respectively. Both hydrogen and helium discharge data are included in the figure because no significant difference in the confinement properties have been observed. The density ranges are restricted to 4-5 x 10$^{19}m^{-3}$ for I_p=2 MA case and 3.4-4.0 x 10$^{19}m^{-3}$ for I_p=1.5 MA case because the stored energy has a strong dependence on the plasma density in the ohmic discharges. The total stored energy is compared with the magnetic measurement which is shown in the Appendix. The plasma stored energy follows an off set linear relation with the absorbed power having incremental energy confinement times for the total stored energy τ_{EC}^{inc} (= dW_{TOT}/dP_{abs}) of 86 msec and 83 msec for I_p= 2 MA and 1.5 MA cases, respectively. τ_{EC}^{inc} for I_p = 1.5 MA H^0 neutral injection case is larger than that of D^0 injected TFTR result [12]. τ_{EC}^{inc} is relatively insensitive to plasma current. Fig. 6 shows thermal and total stored energies W_s and W_{TOT} as a function of $\overline{n}_e$ for I_p= 2MA discharges. The experimental data between P_{abs} =13.4-16.9 MW are converted to P_{abs} =15 MW in this figure. The incremental energy confinement time for thermal component τ_E^{inc} (=dW_s/dP_{abs}) is almost independent of $\overline{n}_e$ and is 60 msec. It should be noted that we do not subtract the charge exchange loss for the definition of τ_E^{inc} while TFTR group subtracted the charge exchange loss for the definition of heating power P_{heat} [19]. If we add the calculated beam stored energy, the total stored energy is almost independent of n_e and the global energy confinement time τ_{EG} is 120 msec. Therefore, we expect that τ_{EC}^{inc} is more than 100 msec in low density regime although the energy confinement time for thermal component is fairly lower than that in high density regime. Fig.7 shows a similar plot for I_p = 1.5 MA and 1 MA cases. The incremental energy confinement times for the thermal component τ_E^{inc} are 60 msec for both I_p= 1.5 and 1.0 MA cases as seen from the figure. The experimental data between P_{abs} = 9.1-10.9 MW are converted to P_{abs} =10MW for I_p=1.5 MA case and the data between 7.4-8.7 MW are converted to P_{abs} = 8 MW, respectively. The total stored energy including the beam component W_T is almost independent of n_e for I_p=1.5 MA case. Density scan for I_p=1 MA discharges is not performed because of the short experimental period.

The incremental energy confinement time for the thermal component is almost independent of I_p and $\overline{n}_e$ which is the same conclusion with JFT-2M results [16]. τ_E^{inc} for H^0 injection is 60 msec and 7 times less than the energy confinement time during the ohmic heating. This ratio τ_E^{OH} / τ_E^{inc} is fairly larger than that of JFT-2M result τ_E^{OH}/τ_E^{inc} =3.2 [31]. The energy confinement time during the ohmic heating has been increased by the favourable size scaling ($\tau_E^{OH} \propto R^2 a$) in large tokamaks [32] . On the other hand, the incremental energy confinement time during the L-mode discharges seems to have less favourable size scaling. For this size scaling part, Shimomura and Odajima [17] proposed as,

$$\tau_E^{inc} = .12\sqrt{m/m_D}\ a_p^2$$

which gives τ_E^{inc} = 64 msec for the experimental conditions in JT-60. This is fairly consistent with the experimental observation.

The energy confinement time $\tau_E\,(=(W_e+W_i)/\ P_{abs})$ decreases down to 100 msec during 20 MW injection from the ohmic heating value(400-500 msec). Fig.8 shows τ_E as a function of P_{abs} .

5.PROFILE CHARACTERISTICS

Fig.9 shows typical example of electron temperature and density profiles for both ohmic and beam heated limiter and divertor discharges. A significant difference in the density profile has been observed between limiter and divertor cases while T_e profile is relatively unchanged. Solid and broken lines in the density profile are n_e profiles obtained by the 4 channel FIR/2mm interferometers and by the Thomson scattering which give good coincidence. Fig.10 shows $n_e(0)/\bar{n}_e$ as a function of $\bar{n}_e$ for hydrogen(OH and NB) and helium(NB) discharges. Extremely flat density profile is realized in high density ohmically heated divertor discharges while more peaked density profile is seen in limiter discharges. A peaked density profile tends to be formed even for the divertor discharges for full size plasmas with minor radius more than 88 cm. This fact indicates the importance of the plasma-wall interaction for the appearance of the peaked density profile. At least we can say that strong particle inward flow [33] caused by the ion mixing mode [34] is absent in high density divertor discharges in JT-60.

Contrary to the density profile, the electron temperature profile tends to keep a bell-shaped form. Fig.11 shows $T_e(0)/\langle T_e\rangle$ for ohmic and beam heated discharges as a function of $1/q_{eff}$ with restricted increased by the favourable size scaling ($\tau_E^{OH} \propto R^2 a$) in large tokamaks [32] . On the other hand, the incremental energy confinement time during the L-mode discharges seems to have less favourable size scaling. For this size scaling part, Shimomura and Odajima [17] proposed as,

$$\tau_E^{inc} = .12\sqrt{m/m_D}\ a_p^2$$

which gives τ_E^{inc} = 64 msec for the experimental conditions in JT-60. This is fairly consistent with the experimental observation.

The energy confinement time $\tau_E\,(=(W_e+W_i)/\,P_{abs})$ decreases down to 100 msec during 20 MW injection from the ohmic heating value(400-500 msec). Fig.8 shows τ_E as a function of P_{abs} .

5.PROFILE CHARACTERISTICS

Fig.9 shows typical example of electron temperature and density profiles for both ohmic and beam heated limiter and divertor discharges. A significant difference in the density profile has been observed between limiter and divertor cases while T_e profile is relatively unchanged. Solid and broken lines in the density profile are n_e profiles obtained by the 4 channel FIR/2mm interferometers and by the Thomson scattering which give good coincidence. Fig.10 shows $n_e(0)/\bar{n}_e$ as a function of $\bar{n}_e$ for hydrogen(OH and NB) and helium(NB) discharges. Extremely flat density profile is realized in high density ohmically heated divertor discharges while more peaked density profile is seen in limiter discharges. A peaked density profile tends to be formed even for the divertor discharges for full size plasmas with minor radius more than 88 cm. This fact indicates the importance of the plasma-wall interaction for the appearance of the peaked density profile. At least we can say that strong particle inward flow [33] caused by the ion mixing mode [34] is absent in high density divertor discharges in JT-60.

Contrary to the density profile, the electron temperature profile tends to keep a bell-shaped form. Fig.11 shows $T_e(0)/\langle T_e\rangle$ for ohmic and beam heated discharges as a function of $1/q_{eff}$ with restricted density range. The measured $T_e(0)/<T_e>$ is compared with the general inequality $q_{eff}^{.667} < T_e(0)/<T_e>$ (uniform Z_{eff} and spitzer resistivity assumed). Measured $T_e(0)/<T_e>$ values follow this lower bound $q_{eff}^{.667}$ in ohmically heated discharges. Effect of sawteeth broadens this peaking parameter during the neutral beam heating as seen from the figure and we can not see clear correlation with q_{eff}^{-1}. Fig.12 shows $T_e(0)/<T_e>$ as a function of $\bar{n}_e$ for both ohmic and beam heating cases. Although sawteeth effect blurs the tendency, we can see a formation of the broader temperature profile in high density beam heated discharges. However, this profile change is not large enough to reject so called "Temperature Profile Consistency" [18]. Fig.13 shows radial profiles of the NB-supplied particle deposition calculated with the Orbit-Following-Monte-Carlo code and of the energy confinement time for low and high density helium discharges. The core energy confinement is significantly larger than the gross energy confinement time for high density hollow beam deposition cases similar to the TFTR case [19] .

6. TRANSPORT INSIDE THE PLASMA

Convective and conductive energy transports have been analyzed for these discharges. Fig.14 shows the particle diffusion coefficient D and the convective energy loss normalized by the input power at r=2a/3 as a function of input power P_{in} (=P_{abs} -P_{cx}) where P_{cx} is the charge exchange loss power of the fast ion. In this calculation, we estimated the convective energy loss by P_{conv}=3/2nTV and is only 10 % of the total input power although there is no consensus on this convective loss formula [35] . At least we can say that convective energy loss is not a dominant energy loss channel although significant enhancement of D has been observed in these discharges. Fig.15 shows the electron thermal conduction coefficient χ_e and the electron conduction loss power normalized by the input power at r=2/3a as a function of P_{in}. Basically, we assumed $\chi_i=5\chi_i^{NC}$ and some of the experimental data are obtained by using $T_i(0)$ which gives C_i=1-4 for this range of plasma density. As is seen from the figure, about 70-80 % of the heating power is lost through the electron heat conduction.

density range. The measured $T_e(0)/\langle T_e \rangle$ is compared with the general inequality $q_{eff}^{.667} < T_e(0)/\langle T_e \rangle$ (uniform Z_{eff} and spitzer resistivity assumed). Measured $T_e(0)/\langle T_e \rangle$ values follow this lower bound $q_{eff}^{.667}$ in ohmically heated discharges. Effect of sawteeth broadens this peaking parameter during the neutral beam heating as seen from the figure and we can not see clear correlation with q_{eff}^{-1} . Fig.12 shows $T_e(0)/\langle T_e \rangle$ as a function of $\bar{n}_e$ for both ohmic and beam heating cases. Although sawteeth effect blurs the tendency, we can see a formation of the broader temperature profile in high density beam heated discharges. However, this profile change is not large enough to reject so called "Temperature Profile Consistency" [18] . Fig.13 shows radial profiles of the NB-supplied particle deposition calculated with the Orbit-Following-Monte-Carlo code and of the energy confinement time for low and high density helium discharges. The core energy confinement is significantly larger than the gross energy confinement time for high density hollow beam deposition cases similar to the TFTR case [19] .

6.TRANSPORT INSIDE THE PLASMA

Convective and conductive energy transports have been analyzed for these discharges. Fig.14 shows the particle diffusion coefficient D and the convective energy loss normalized by the input power at r=2a/3 as a function of input power P_{in} ($=P_{abs} - P_{cx}$) where P_{cx} is the charge exchange loss power of the fast ion. In this calculation, we estimated the convective energy loss by P_{conv}=3/2nTV and is only 10 % of the total input power although there is no consensus on this convective loss formula [35] . At least we can say that convective energy loss is not a dominant energy loss channel although significant enhancement of D has been observed in these discharges. Fig.15 shows the electron thermal conduction coefficient χ_e and the electron conduction loss power normalized by the input power at r=2/3a as a function of P_{in}. Basically, we assumed $\chi_i = 5\chi_i^{NC}$ and some of the experimental data are obtained by using $T_i(0)$ which gives C_i=1-4 for this range of plasma density. As is seen from the figure, about 70-80 % of the heating power is lost through the electron heat conduction.

7. CONCLUSION

The energy confinement characteristics during the initial neutral beam heating has been analyzed by the time independent radial transport analysis code using the radial profile of the electron temperature and central ion temperature. The global energy confinement time follows an off set linear relation with absorbed power and the incremental energy confinement time for the thermal component is almost independent of $\bar{n}_e$ and I_p. A remarkable difference in the density profile has been observed between limiter and divertor discharges. The density profile is extremely flat in high density divertor discharges while more peaked density profile has been observed in the limiter discharges. Contrary to the density profile, the temperature profile shape is rather tight although some broadening has been observed in high density hollow beam deposition cases. The power balance studies shows that the convective energy loss is only 10 % of the total energy loss while the electron conduction loss goes up to 70-80 % of the energy loss.

ACKNOWLEDGEMENTS

One of the authors(M.K.) would like to express his appreciation to Dr.Odajima for his comments on JFT-2M experiments.

The authors would like to express their appreciation to Drs. S.Mori and K.Tomabechi for their continued leadership and support.

7. CONCLUSION

The energy confinement characteristics during the initial neutral beam heating has been analyzed by the time independent radial transport analysis code using the radial profile of the electron temperature and central ion temperature. The global energy confinement time follows an off set linear relation with absorbed power and the incremental energy confinement time for the thermal component is almost independent of $\bar{n}_e$ and I_p. A remarkable difference in the density profile has been observed between limiter and divertor discharges. The density profile is extremely flat in high density divertor discharges while more peaked density profile has been observed in the limiter discharges. Contrary to the density profile, the temperature profile shape is rather tight although some broadening has been observed in high density hollow beam deposition cases. The power balance studies shows that the convective energy loss is only 10 % of the total energy loss while the electron conduction loss goes up to 70-80 % of the energy loss.

ACKNOWLEDGEMENTS

One of the authors(M.K.) would like to express his appreciation to Dr.Odajima for his comments on JFT-2M experiments.

The authors would like to express their appreciation to Drs. S.Mori and K.Tomabechi for their continued leadership and support.

References

[1] Yoshikawa,M.,Nucl. Fusion 25(1085)1081.

[2] Yoshikawa,M. and JT-60 team, Plasma Physics and Controlled Nuclear Fusion Research, IAEA, Vienna, 1986, IAEA-CN-47/A-I-1.

[3] JT-60 team presented by M.Nagami, Plasma Physics and Controlled Nuclear Fusion Research, IAEA, Vienna, 1986, IAEA-CN-47/A-II-2.

[4] JT-60 team presented by H.Takeuchi, Plasma Physics and Controlled Nuclear Fusion Research, IAEA, Vienna, 1986, IAEA-CN-47/A-IV-3.

[5] JT-60 team presented by T.Imai, Plasma Physics and Controlled Nuclear Fusion Research, IAEA, Vienna, 1986, IAEA-CN-47/K-I-2.

[6] JT-60 team presented by M.Yoshikawa, Plasma Physics and Controlled Fusion, 28(1986)165.

[7] JT-60 team presented by S.Tsuji, in Controlled Fusion and Plasma Physics(12th Europ.Conf.Budapest,1985) PartI(1985)375.

[8] JT-60 team presented by S.Tamura, Plasma Physics and Controlled Fusion ,28(1986)1377.

[9] JT-60 team presented by H.Kishimoto, to be published in J. Nucl. Mater.

[10] Goldston,R.J.,Plasma Physics and Controlled Fusion 26 (1084)87.

[11] Kaye,S.M.,Goldston,R.J., Nucl. Fusion 25(1985)65.

[12] Hawryluk,R.J.,Arunasalam,V.,Bell, M.G.,Bitter,M.,Blanchard,W.R. et al., Plasma Physics and Controlled Nuclear Fusion Research, IAEA,Vienna (1986) IAEA-CN-47/A-I-3.

[13] The JET Team(presented by P.H.Rebut),ibid,IAEA-CN-47/A-I-2.

[14] Burrell,K.H.,Prater,R.,Ejima,S., Angel,T.,Armentrout,C.J. et al.,in Plasma Physics and Controlled Nuclear Fusion Research(Proc. 10th Conf., London, 1984) IAEA,Vienna Vol.I(1985)131.

[15] DeBoo,J.C.,Burrell,K.H., Ejima,S.,Kellman,A.G.,Ohyabu,N. et al.,Nucl.Fusion 26(1986) 211.

[16] Odajima,K.,Hoshino,K.,Kasai, S.,Kawakami,T.,Kawashima,H. et al.,Phys.Rev.Lett.57(1986)2814.

[17] Shimomura,Y.,Odajima,K., 'Scaling of Incremental Energy Confinement Time of L-mode Plasma and Comments on Improved Confinement in Tokamaks.',JAERI-M 86-128 (1986).

[18] Coppi,B.,Comments Plasma Phys. and Contr. Fusion 5(1980)201.

[19] Murakami,M.,Arunasalam,V.,Bell, J.D.,Bell,M.G.,Bitter,M. et al.,Plasma Physics and Controlled Fusion 28(1986)17.

[20] Speth,E.,Eberhagen,A.,Gehre,O., Gernhardt,I.,Janeschitz,G. et al., in Controlled Fusion and Plasma Physics(12th Europ. Conf. Budapest,1985)Part II(1985)284.

[21] Arai,T.,Yamamoto,M.,Akino,N., Kodama,K.,Nakamura,H. et al.,to be published in J. Nucl. Mater.

[22] Kikuchi,M.,Ninomiya,H., Yoshino,R.,Seki,S.,to be published in Nucl. Fusion.

[23] Hosogane,N.,Ninomiya,H., Seki,S.,Nucl. Fusion 26(1986)657.

[24] Ninomiya,H.,Hosogane,N., Kikuchi,M.,Yoshino,R.,Seki,S. et al.,Proc. 11th Symp. Fusion Engineering (Austin,USA)Nov.18-22,1985.

[25] Hirayama,T.,Shimizu,K.,Tani,K., Kikuchi,M.,to be published in JAERI-M.

[26] Wieland,R.M.,Howe,H.C., Lazarus,E.A.,Murakami,M.,Thomas,C.E., Nucl. Fusion 23(1983)447.

[27] Tsuji,S.,Hayashi,K.,Yoshida,H., Hosogane,N.,Kikuchi,M. et al, 'MHD equilibrium analysis method of JT-60 based on magnetic measurement' ,JAERI-M 86-006(1986).

[28] Swain,D.W.,Neilson,G.H., Nucl. Fusion 22(1982)1015.

[29] Tani,K.,Azumi,M.,Ohtsuka,M., Kishimoto,H.,Tamura,S.,Heating in Toroidal Plasma (Proc. Joint Varenna-Grenoble Int. Symp. 1978), Vol.1(1978)31.

[30] Chang,C.S.,Hinton,F.L., Phys. Fluids 25(1982)1493.

[31] Odajima,K.,Funahashi,A., Hoshino,K.,Kasai,S.,Kawakami,T. et al., Plasma Physics and Controlled Nuclear Fusion Research, IAEA,Vienna (1986) IAEA-CN-47/A-III-2.

[32] Efthimion,P.C.,Bell,M.,Blanchard, W.R.,Bretz,N.,Cecci,J.L. et al., Phy. Rev. Lett. 52(1984)1492.

[33] Coppi,B.,Sharky,N., Nucl. Fusion 21(1981)1363.

[34] Coppi,B.,Spicht,C., Phys.Rev.Lett.41(1978)551.

[35] Hawryluk,R.J.,'An Empirical Approach to Tokamak Transport',in Proc. of the Course in Physics Close to Thermonuclear Conditions, (Varenna, Italy), EUR-FU-BRU/XII/ 476/80.

Appendix

Plasma stored energy during the neutral beam heating has been estimated by the equilibrium field measurement. Shafranov Λ measured by the equilibrium is expressed as follows,

$$\Lambda = \beta_p^{eq.} + \frac{\ell_i}{2}$$

where $\beta_p^{eq} = \mu_0(\langle P_{/\!/} + P_{\perp} \rangle)/B_p^2$ and l_i is the internal inductance, respectively. If we assume that the internal inductance does not change during the beam heating, we can estimate the plasma stored energy as follows,

$$W_T' = W_s^{OH} + \Delta W_{NB}'$$

$$W_s^{OH} = \text{(see section 4.)}$$

$$\Delta W_{NB}' = 0.471\ R_p(\mathrm{m}) I_p^2(\mathrm{MA})\ \Delta\Lambda\ (\mathrm{MJ})$$

$$W_T' \equiv W_e + W_i + \frac{3}{4} W_{b\perp}$$

where we used the pararell beam pressure is negligible in JT-60. This plasma stored energy by the equilibrium measurement W' is compared with the kinetic measurement as shown in Fig.A1. Relatively good agreement between these measurements are found.

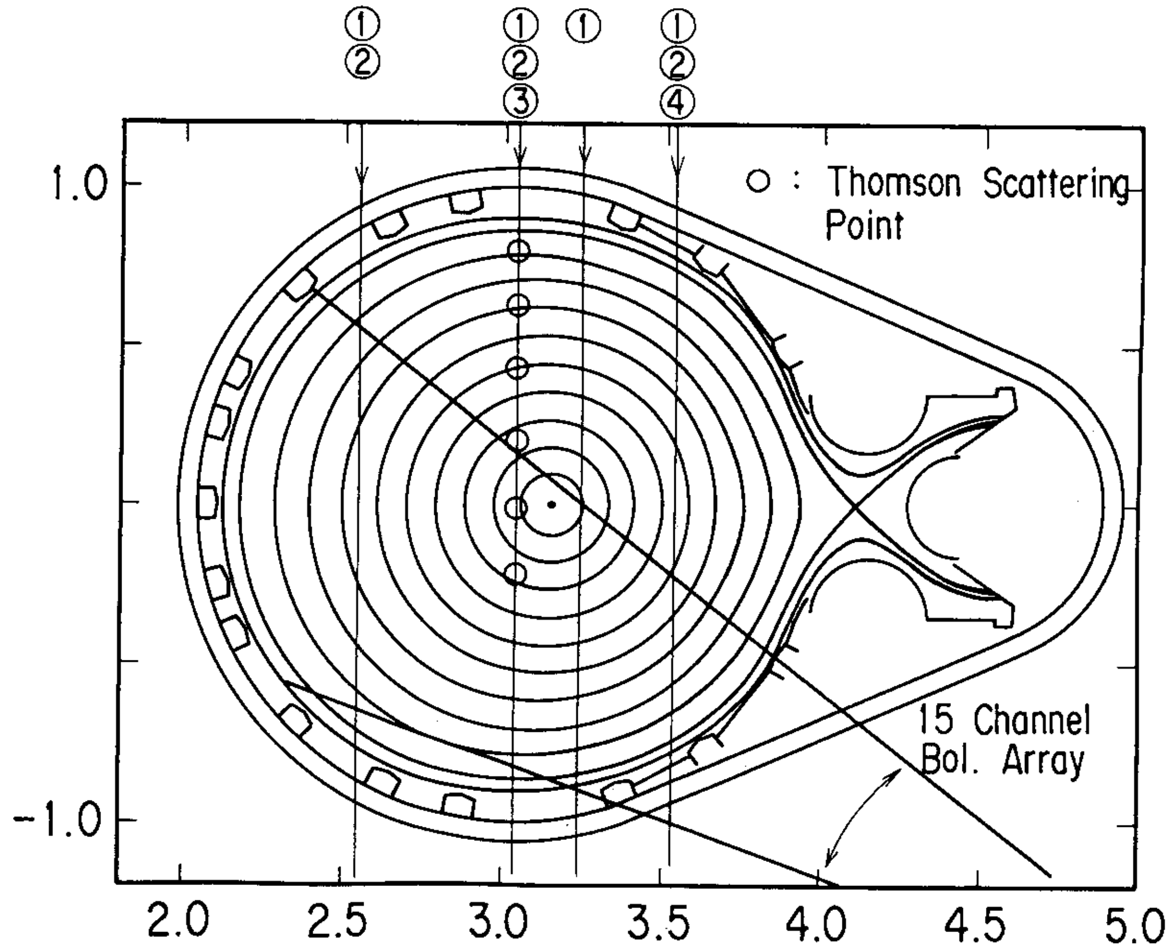

Fig. 1 Diagnostics available for confinement analysis in JT-60. The spacial location of the Thomson scattering points are shown by (o). 15 channel bolometer array viewing small major radius side gives total radiation and 3 channel bolometers viewing 3 vertical lines (2) gives the degree of the poloidal asymmetry. 4 channel interferometers viewing vertical lines are used to estimate the density profile which is also checked by the Thomson scattering. $T_i(0)$ is measured by the doppler broadening of T_i^{XXI} K_α line, charge exchange (3) and Rutherford scattering of active H_e beam (5). Faraday rotation is measured to estimate the density averaged vertical field (4). Particle confinement time is estimated by the 3 channel H_α detectors (2).

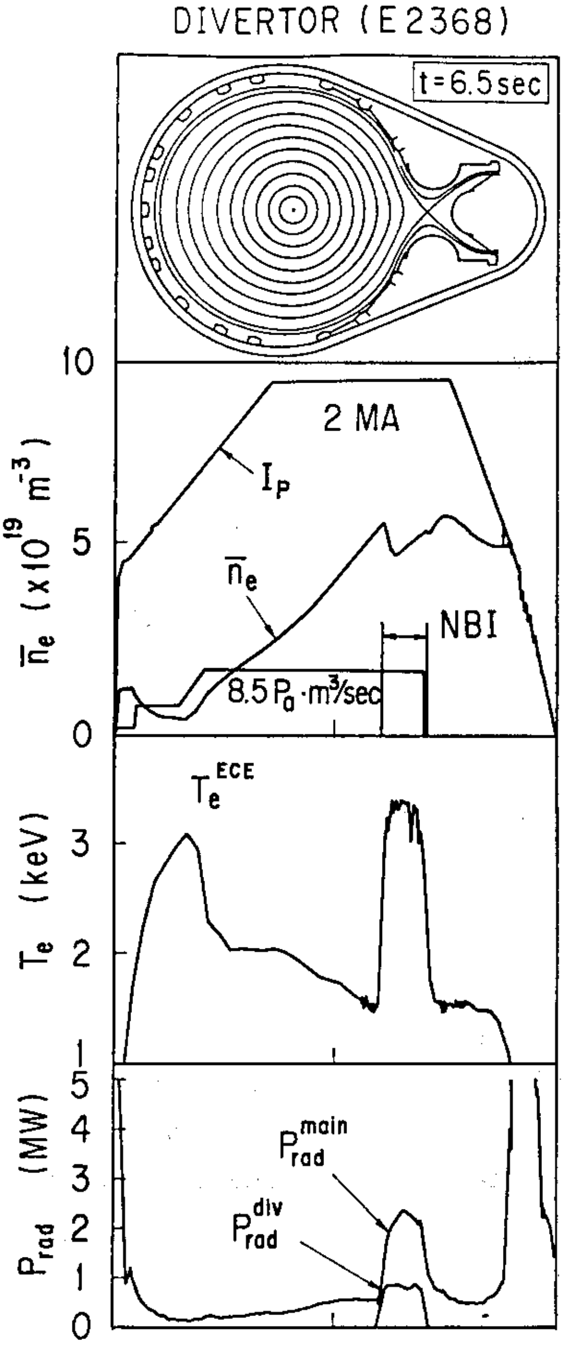

Fig. 2 Typical discharge characteristics during the high power beam heating of divertor discharge in JT-60.

Analysis Procedure

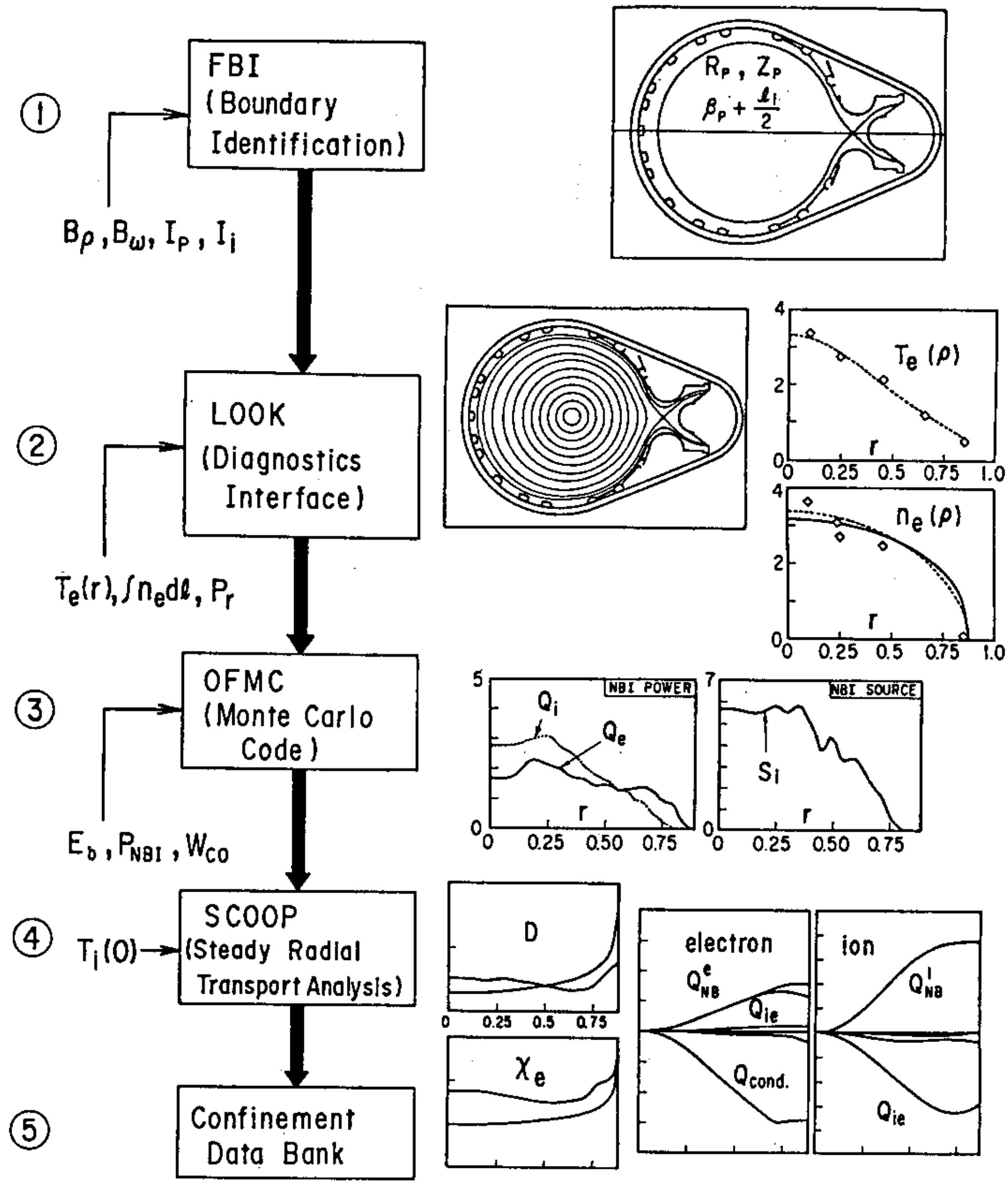

Fig. 3 Rough scketch of the time independent radial transport analysis procedure during the beam heating in JT-60.

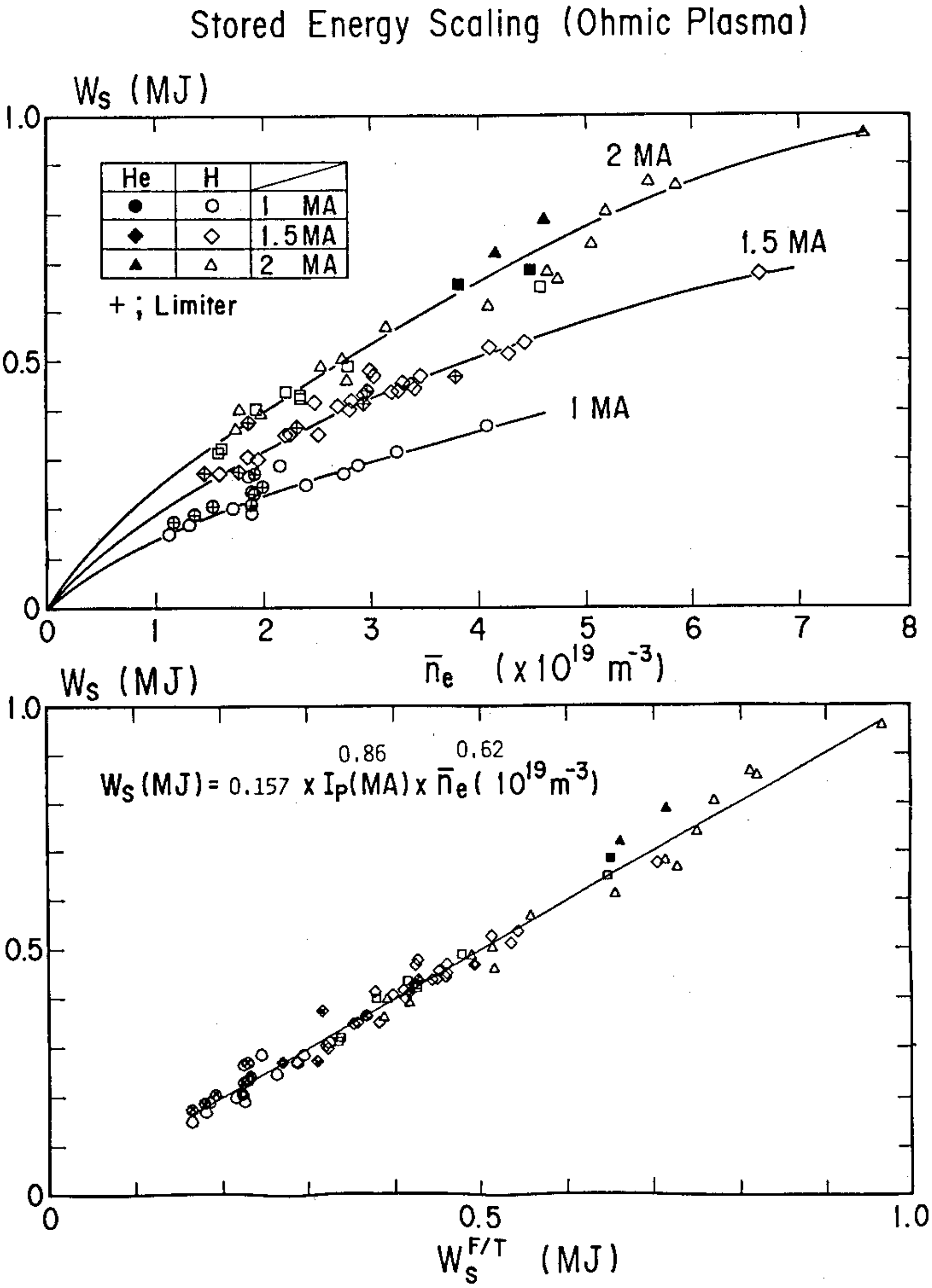

Fig. 4 Plasma stored energy during the ohmic heating as a function of n_e and I_p .

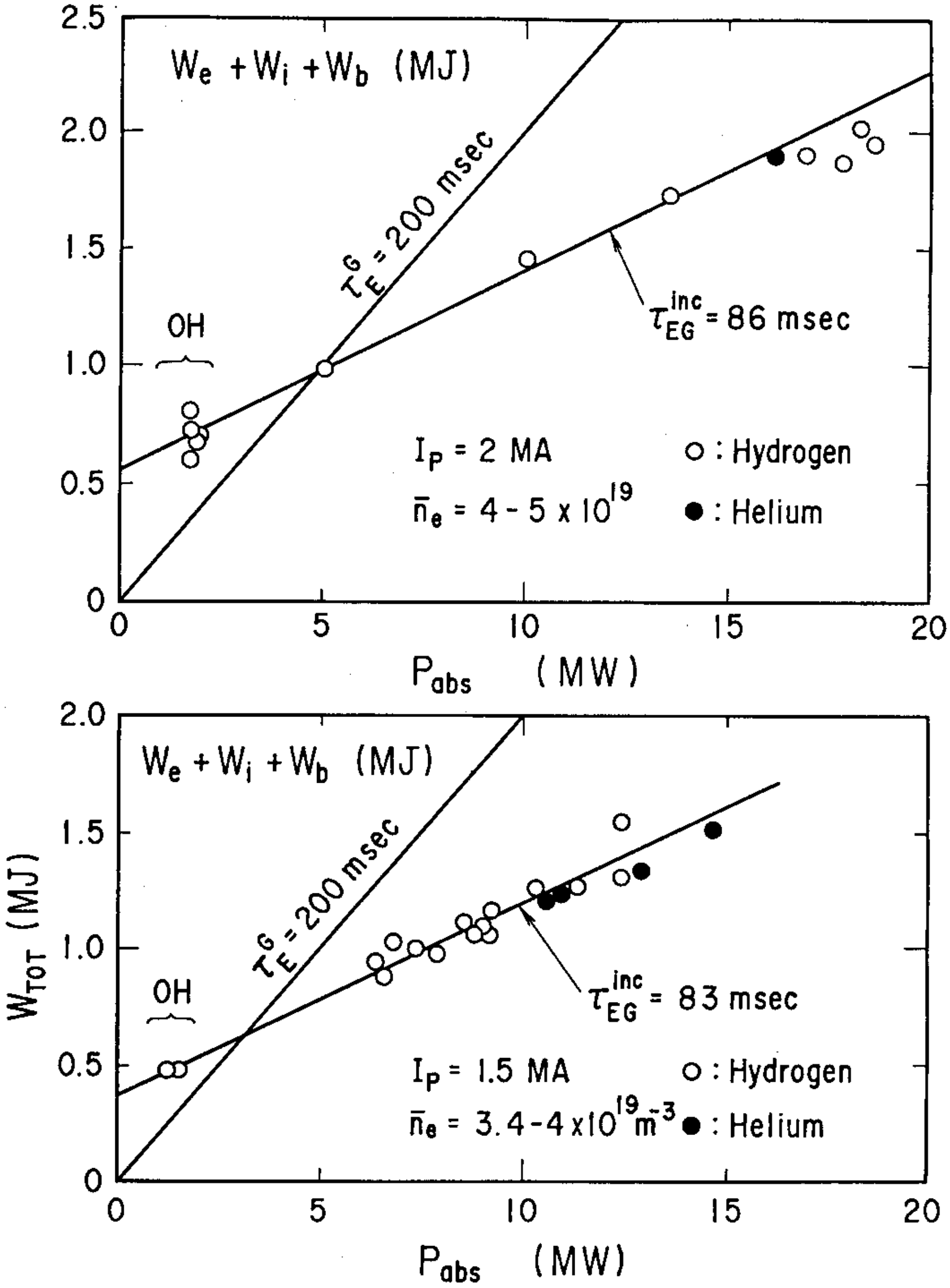

Fig. 5 Total stored energy for 2 and 1.5 MA divertor power scan with restricted density range. Total stored energy increases linearly with P_{abs} .

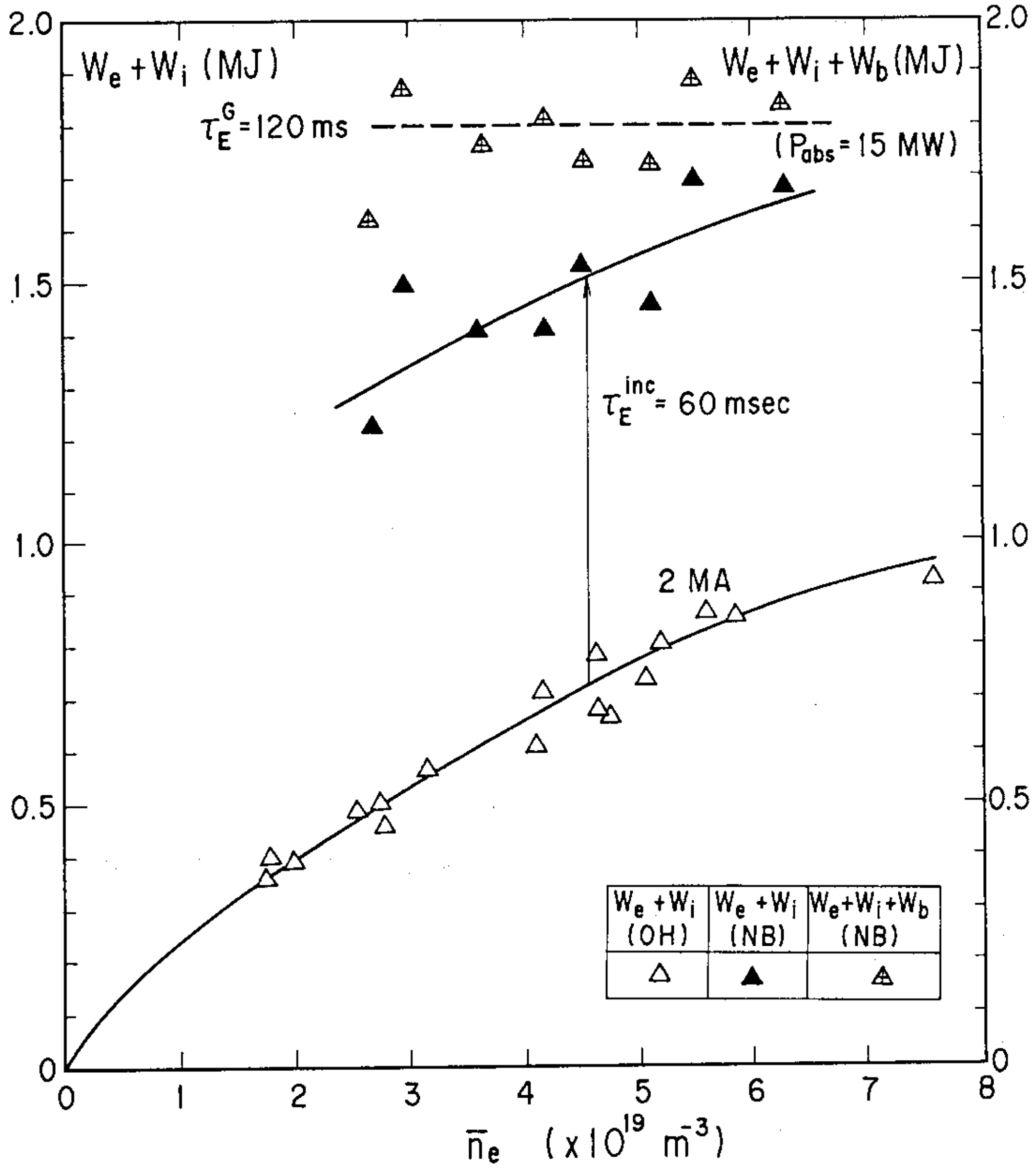

Fig. 6 Total and thermal stored energies for 2 MA density scan. Plasma stored energy is almost doubled with P_{abs} =15 MW. The increase of the thermal stored energy is almost independent of n_e while the increase of the total stored energy depends on n_e.

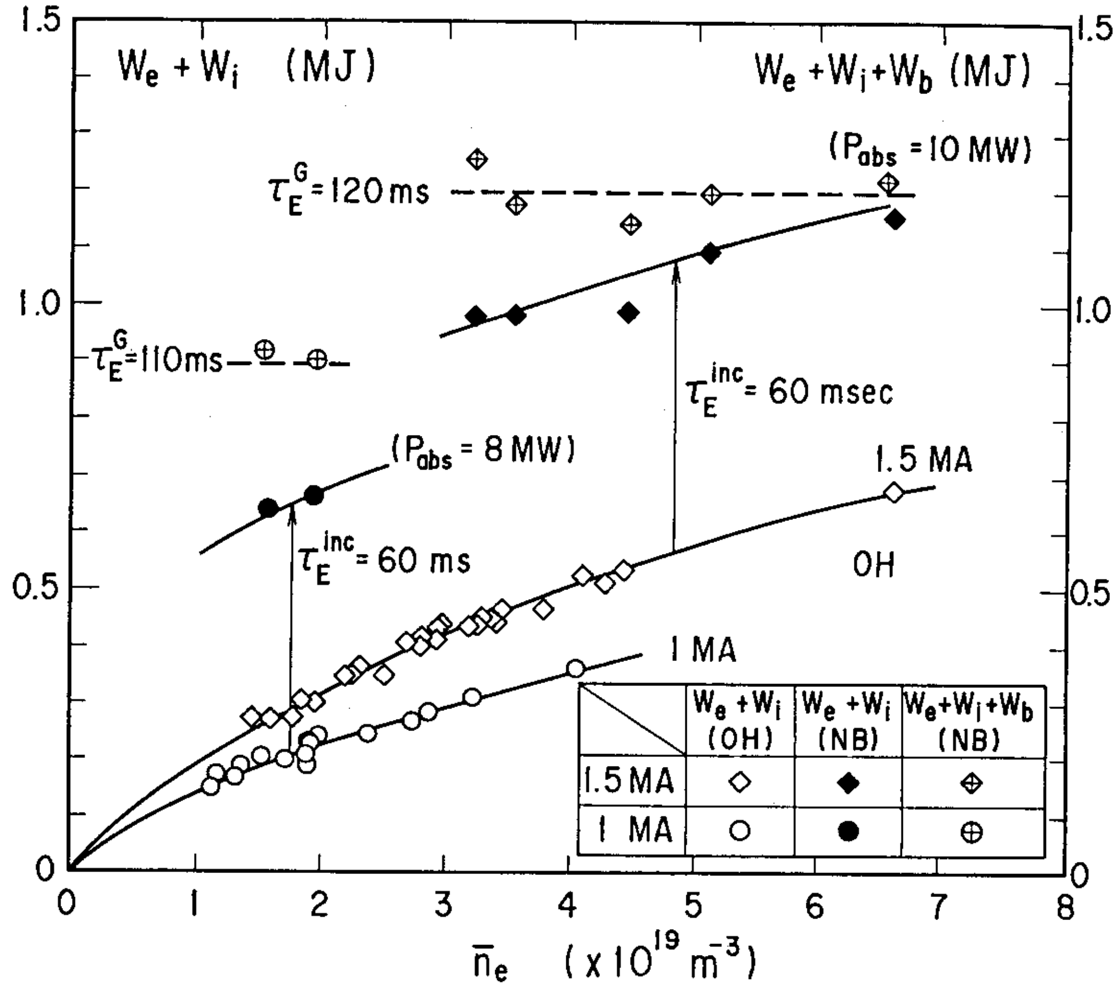

Fig. 7 Total and thermal stored energies for 1.5 and 1 MA density scan. The incremental energy confinement time for thermal components is almost independent of I_p.

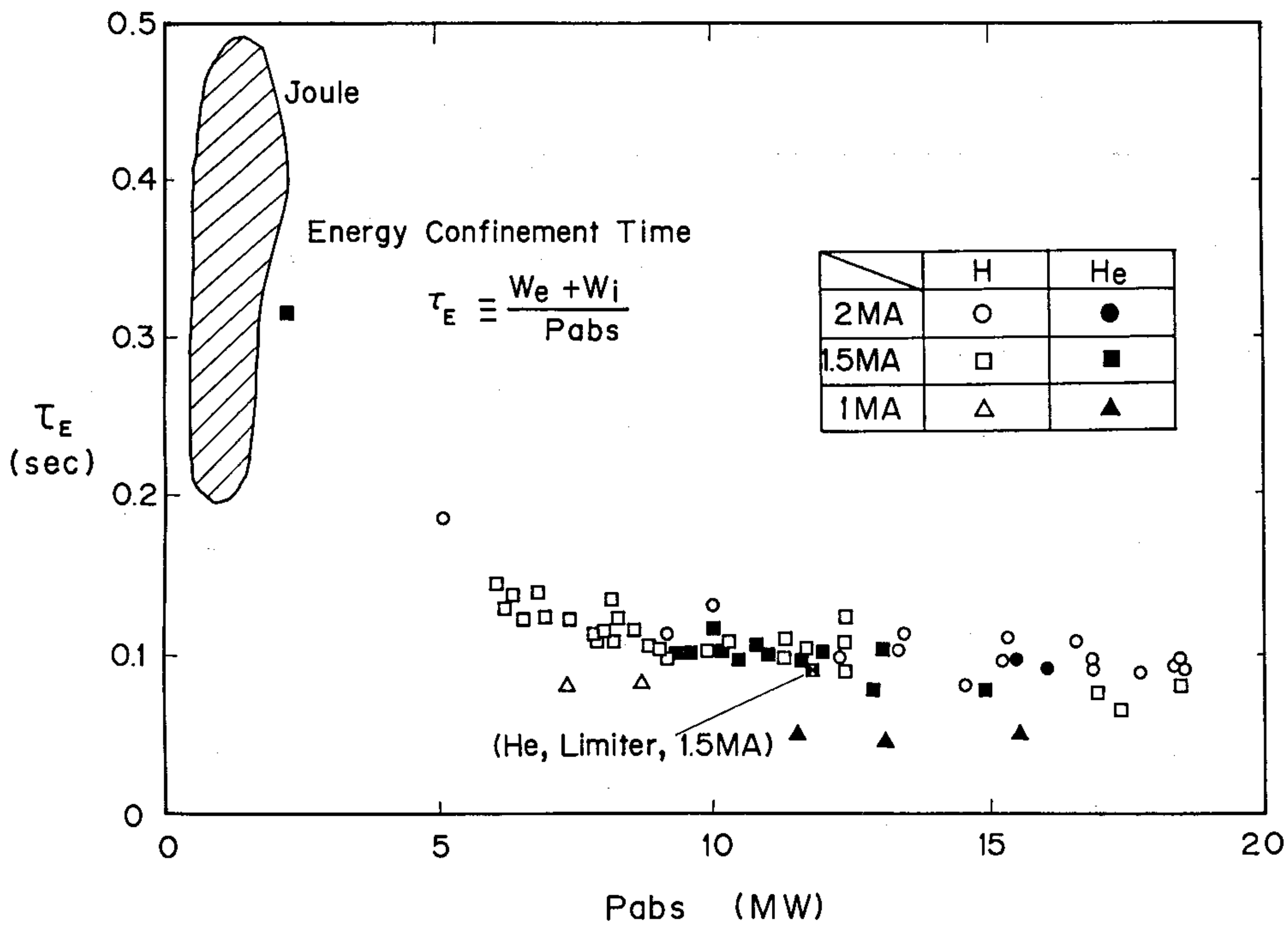

Fig. 8 Energy confinement time as a function of plasma absorbed power for various plasma current.

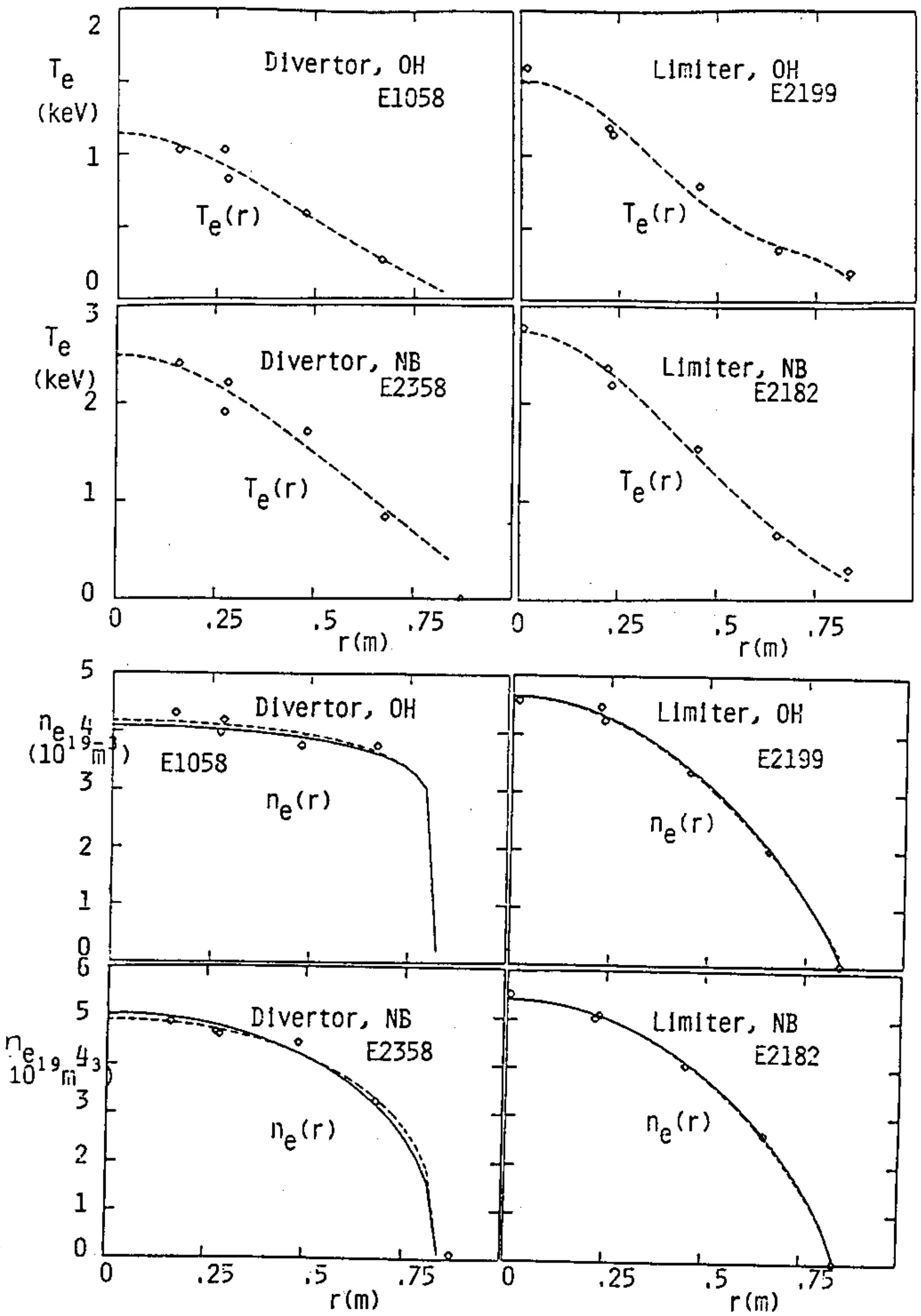

Fig. 9 Electron temperature and density profiles for both ohmic and beam heated divertor and limiter discharges. Functional forms given by eqn. (1) are assumed and the unknown parameters are obtained by the least square fit to the experimental data.

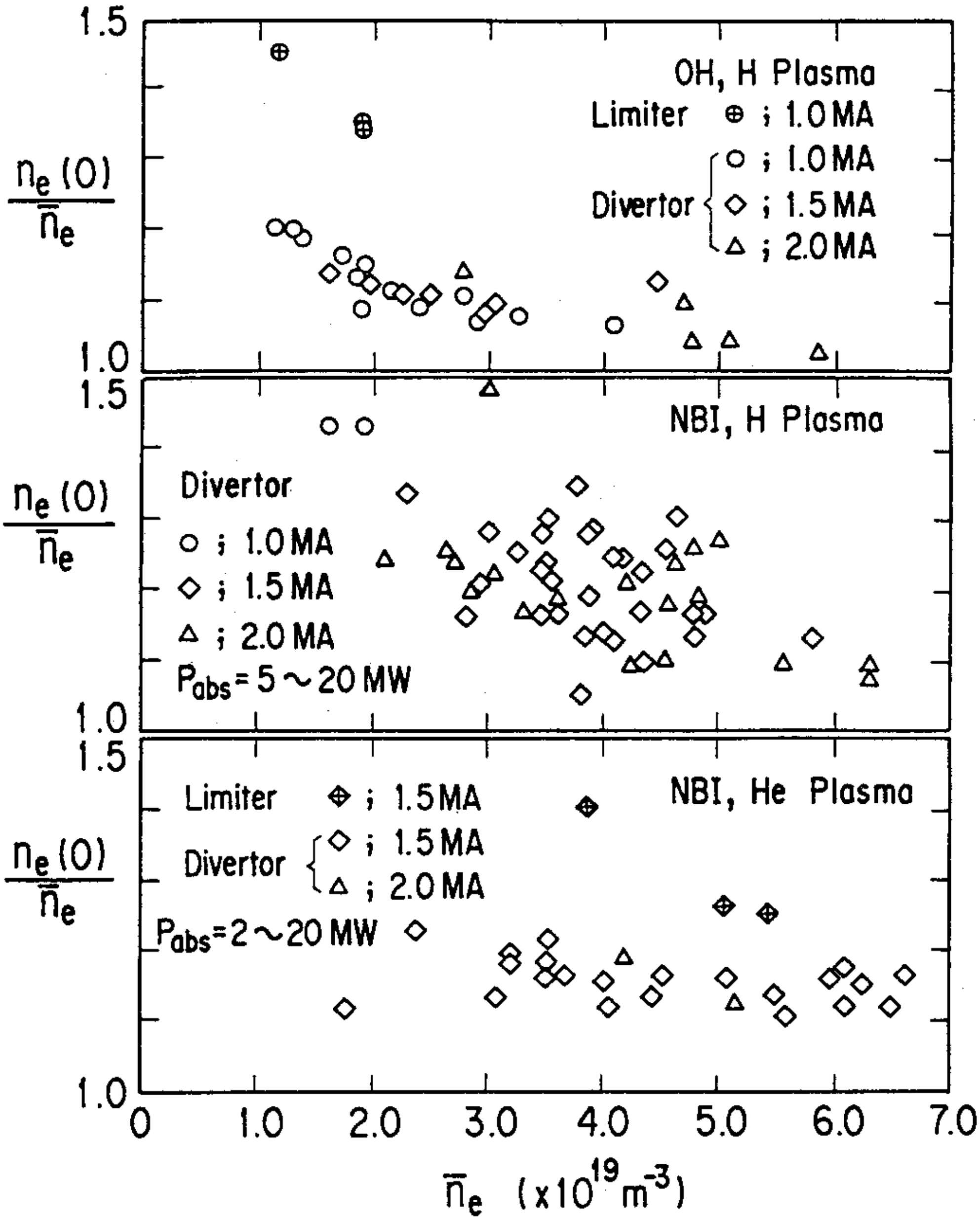

Fig.10 Density peaking parameter $n_e(0)/\bar{n}_e$ for hydrogen (OH and NB) and helium(NB) discharges as a function of $\bar{n}_e$. Both divertor and limiter cases are shown in the figure.

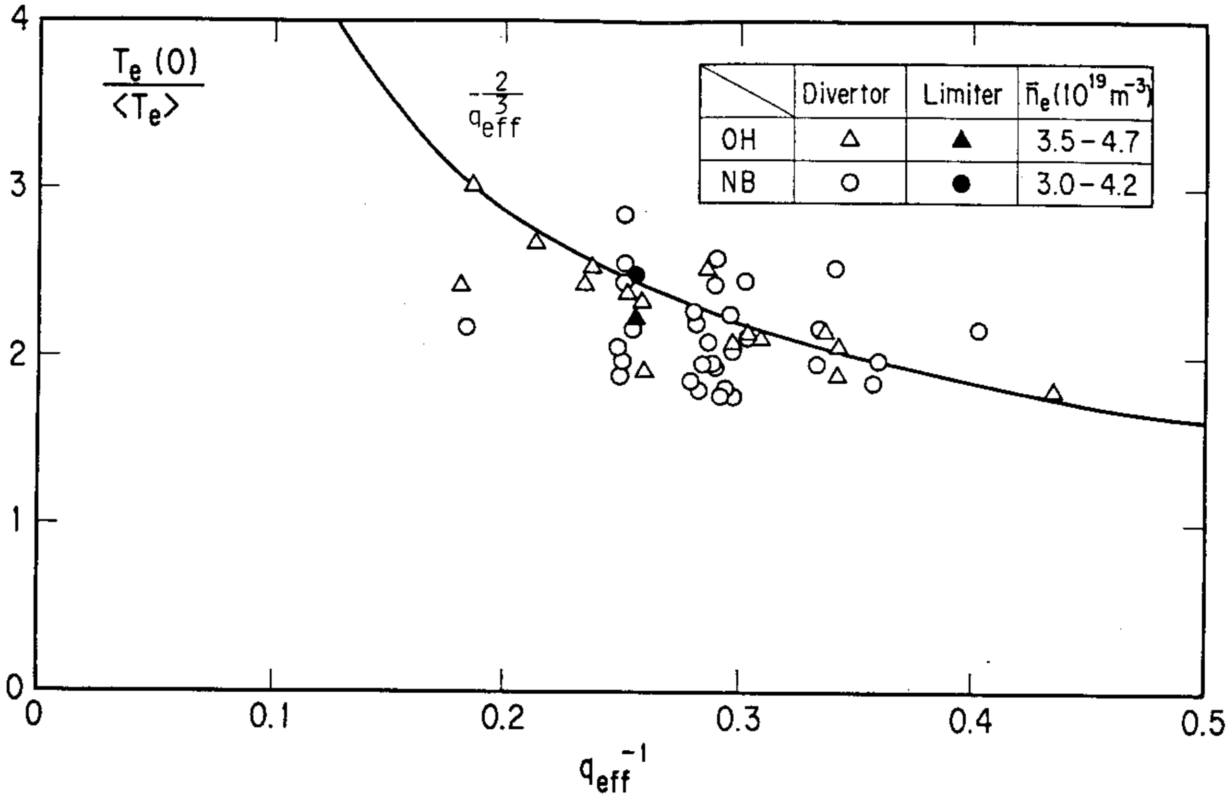

Fig.11 Temperature peaking parameter $T_e(0)/\langle T_e\rangle$ for ohmic and beam heating cases for restricted density range.

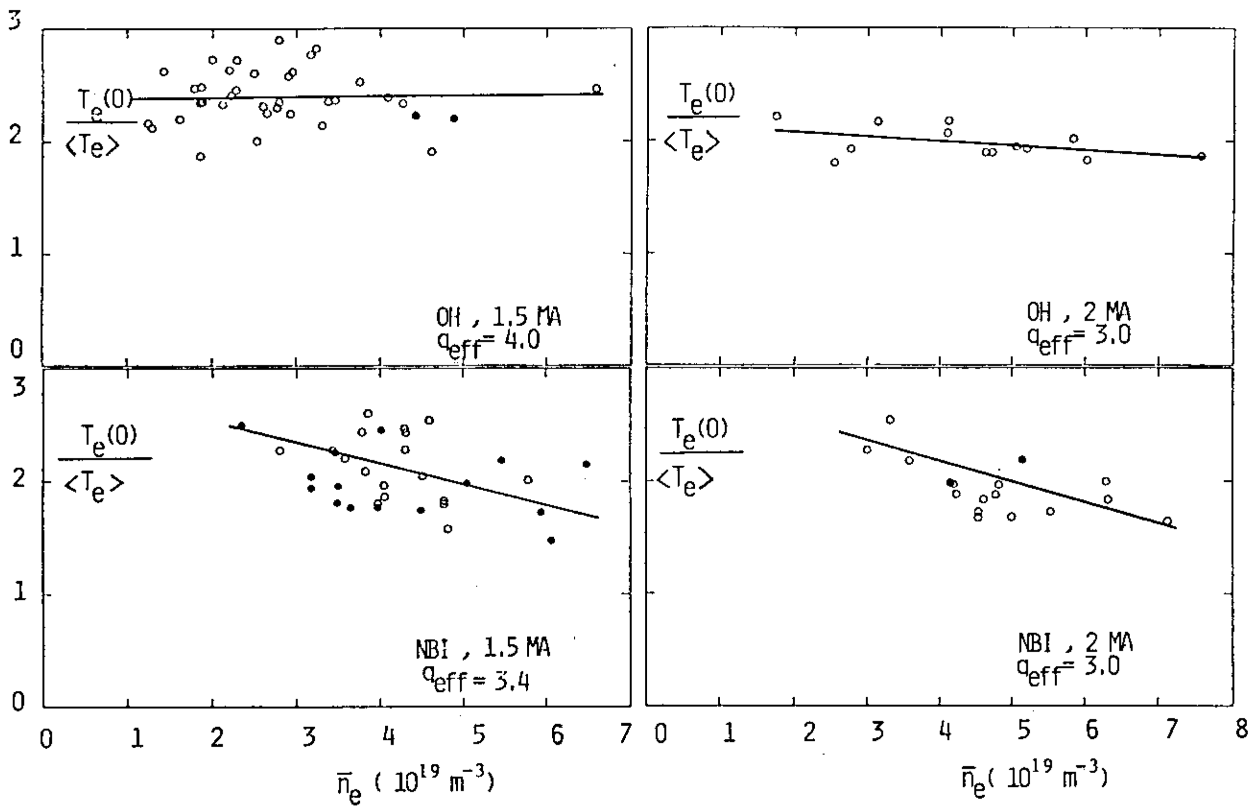

Fig.12 Temperature peaking parameter $T_e(0)/\langle T_e\rangle$ as a function of n_e for both ohmic and beam heating cases for restricted q_{eff} range.

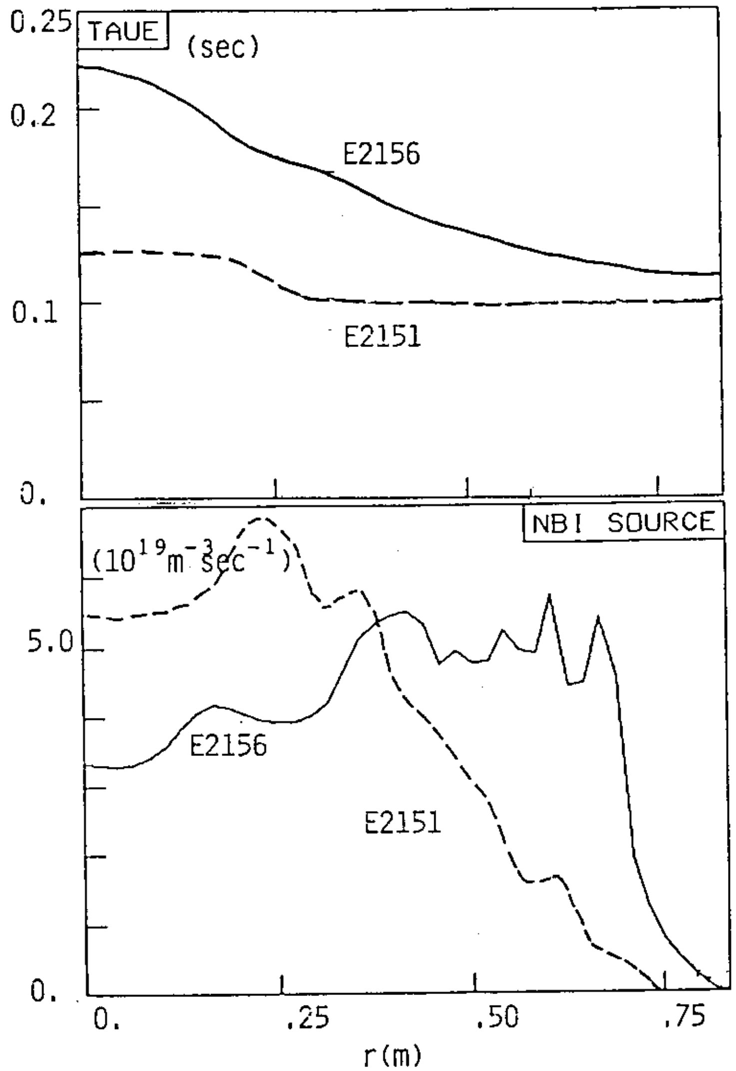

Fig.13 Radial profiles of the energy confinement time and the NB-supplied particle source profiles for low and high density helium discharges.

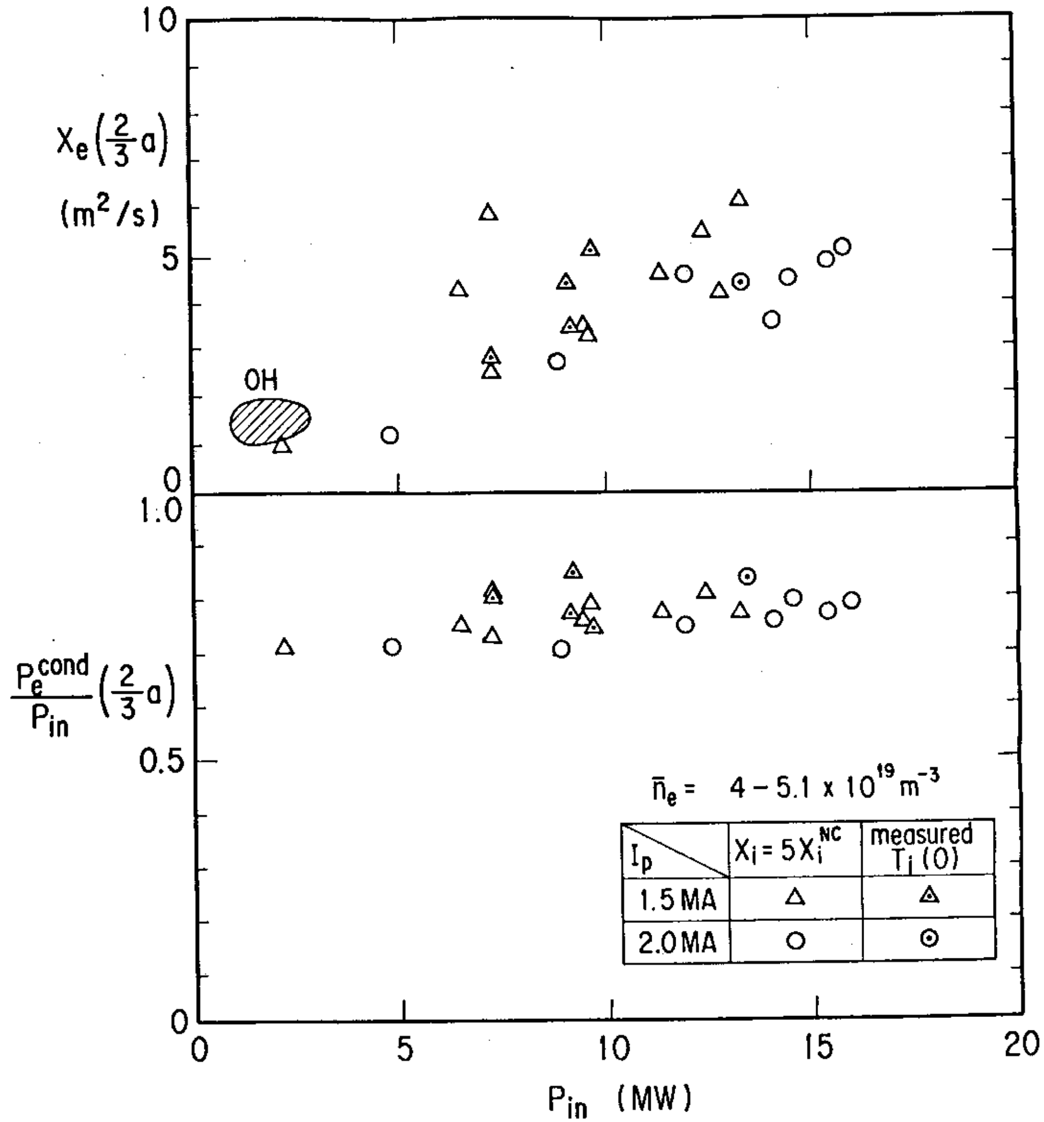

Fig.14 Particle diffusion coefficient D and the convective energy loss P_{conv} normalized by the input power P_{in} at r = 2a/3 as a function of total input power for I_p = 2 MA divertor discharges.

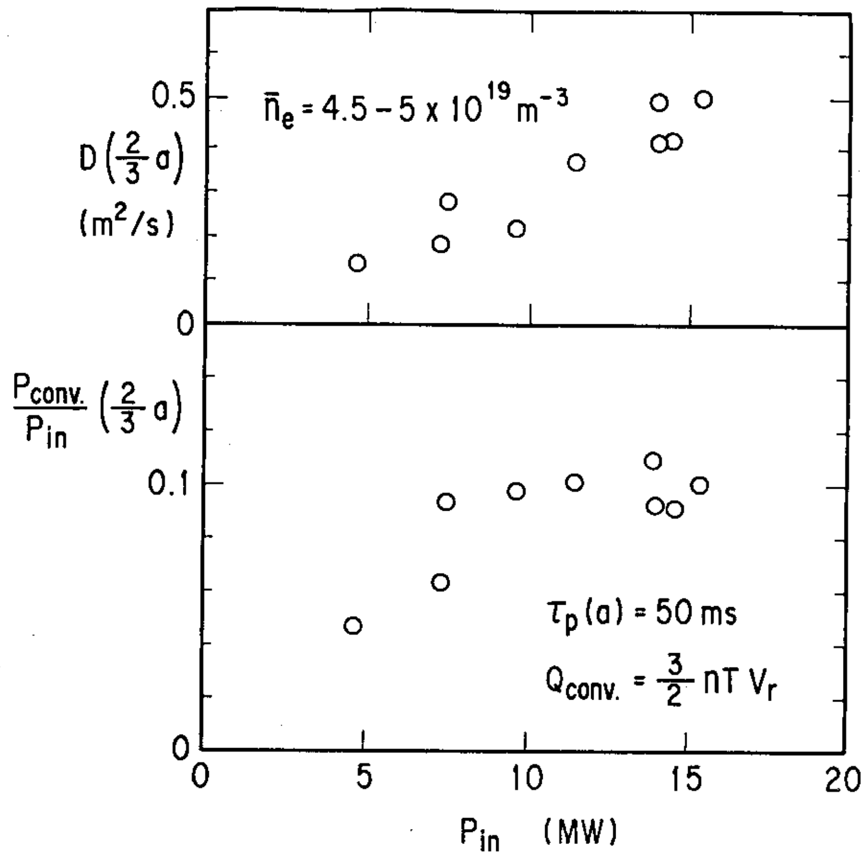

Fig.15 Electron thermal conduction coefficient χ_e during the beam heating for I_p=1.5 and 2 MA discharges with restricted density range as a function of input power. Charge exchange loss is subtracted from the absorbed power by assuming τ_p(a)=50 msec.

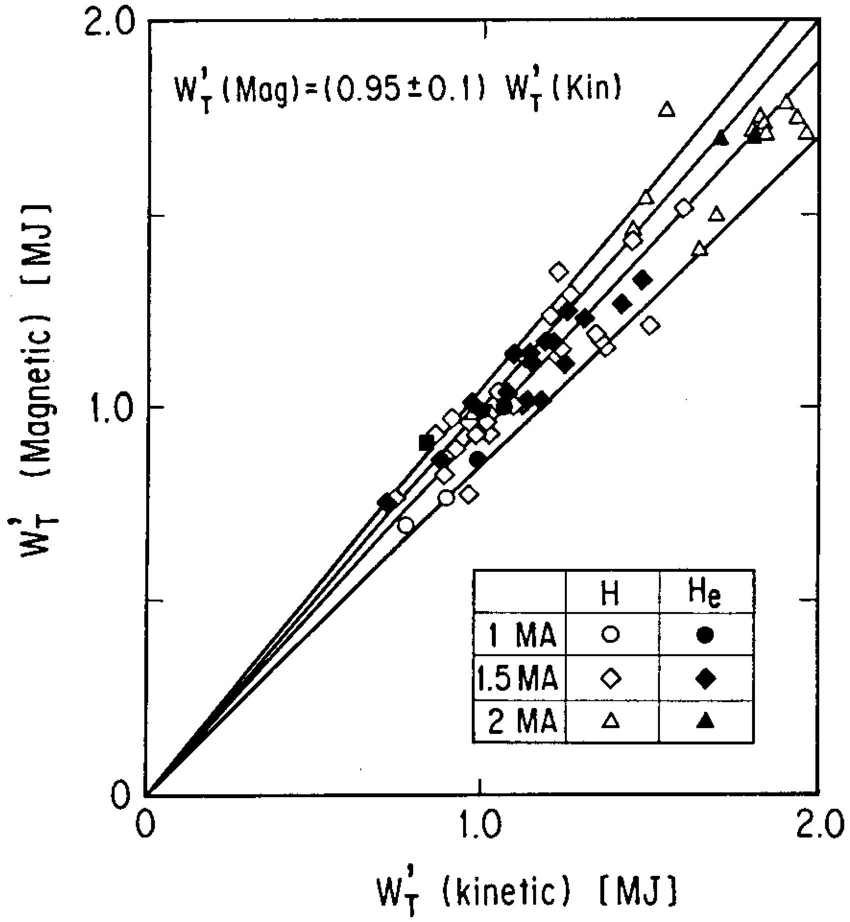

Fig.A1 Comparison of the plasma stored energy W_T' between equilibrium measurement and kinetic measurement.